MULTI-SCALE APPROACH FOR RETINAL VESSEL SEGMENTATION USING MEDIALNESS FUNCTION

Elahe Moghimirad[1], Seyed Hamid Rezatofighi[1], Hamid Soltanian-Zadeh[1 2]

[1]Control and Intelligent Processing Center of Excellence, Department of Electrical and Computer Engineering, Faculty of Engineering, University of Tehran, Tehran, Iran
[2]Image Analysis Lab., Department of Radiology, Henry Ford Hospital, Detroit, Michigan, USA
Emails: {e.moghimirad, h.tofighi}@ece.ut.ac.ir, hszadeh@ut.ac.ir, hamids@rad.hfh.edu

ABSTRACT

Automated segmentation of retinal vessels in optic fundus images has been the most prevailing effort in many researches during recent years. In this paper, we propose a multi-scale method based on a weighted 2D medialness function. The result of the medialness function is first multiplied by the eigenvalues of the Hessian matrix in every pixel of the image in order to extract vessel's medial-lines. Next, by extracting the centerlines of vessels and estimation of radius of vessels, the retinal vessels are segmented. Finally, the performance of our proposed method is evaluated by the DRIVE and STARE databases and compared with those of several recent methods.

Index Terms— Retinal vessel segmentation, medialness function, eigenvalue, radius estimation.

1. INTRODUCTION

Assessment of morphological features of retinal veins and arteries, like diameter, length, branching angle, and tortuosity as crucial indicators reveals preliminary symptoms of many systemic diseases [1]. Thus, the measurement and recognition of exact location of retinal blood vessels has diagnostic relevance for the ophthalmologists. However, because of multifarious nature of the vascular network, manual tracking of retinal vessels is arduous task and suffers from variability of diagnostic results due to both of the inter-observer and intra-observer variations. Therefore, automated segmentation of retinal vessels in optic fundus images has been the most prevalent effort in many researches during recent years.

According to [2], automatic retinal segmentation methods generally fall into three categories as tracking methods, kernel-based and classifier-based methods. For each category, several algorithms have been proposed in [3]-[7]. In [3], an algorithm as a tracking method has been presented which is initialized by a generalized morphological order filter to determine approximate vessels centerlines and uses a "Ribbon of Twins" (ROT) active contour model for segmenting and measuring retinal vessels. Moreover, two classifier-based methods have been introduced in [4] and [5]. Soares *et al.* [4] propounded that feature vectors can be extracted from a two-dimensional Gabor wavelet transform and the pixel's intensity and a Gaussian mixture model classifier can be used for classification. Better results have been obtained in [5] where two line operators are used to extract the feature vectors whilst a Linear Support Vector Machine (LSVM) used as a classifier. The methods introduced by Mendonça *et al.* in [6] and Yan Lam *et al.* in [7] can be classified as kernel-based methods. In [6], Mendonça *et al.* have performed the segmentation of retinal vessels using combination of differential filters (difference of offset Gaussians filters (DoOG filters), used for finding vessel centerline, with an iterative region-growing method that integrates the contents of several binary images for filling vessel segments. In the other one, Yan Lam *et al.* have suggested a scheme based on Laplacian operator for segmenting blood vessels in pathological retinal images. For this purpose, first, the centerlines of vessels are detected using the normalized gradient vector field. Due to existence of noise in pathological regions, noisy objects should be eliminated from the image background. Therefore, as next step, they are pruned according to centerline information.

In this paper, we use a multi-scale technique for segmenting the vessels. We introduce a medialness function, previously used for detection of tubular structures in 3D space [8], for 2D space and weight it with a weighting function to reduce the effect of asymmetric structures. To improve the results of the vessel like structures, the resulting image is multiplied by the eigenvalues of the Hessian matrix. Then, the centerlines of vessels are extracted while the exact boundary of vessels is estimated using the eigenvalues and the result of medialness function. For evaluating the performance of our algorithm, we tested our method on the DRIVE and STARE databases and compared our results with those reported in the most recent articles.

The rest of the paper is organized as follows. In Section 2, we detail the methods used for vessel segmentation. The experimental results are presented and compared with other methods in Section 3. Finally, Section 4 is appropriated to presentation of the conclusions.

2. PROPOSED METHODS

Fig.1 illustrates a block diagram of our proposed scheme. As shown in this figure, the method has two major phases: vessel medial-line detection and vessel reconstruction. Also, each phase is subdivided into several steps whose details are explained in the next sections.

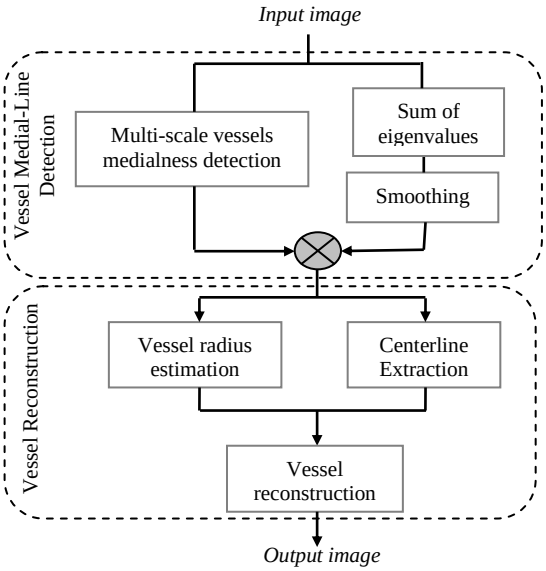

Fig. 1. Block diagram of the proposed vessels segmentation method.

2.1. Vessel Medial-Line Detection

The main purpose of this phase is to extract the medial axis of vessels using a 2D medialness function in several scales and sum of smoothed eigenvalues of the image.

Because of robustness of the medialness function in extracting tubular structures, this function has previously been used to segment these structures in 3D space [8]. In order to apply this function in this application, we define a 2D form of multi-scale medialness function. Moreover, for decreasing the response of asymmetric structures and edges which are usually noise and abnormal regions, the function is constrained by a weighting function as:

$$R_0(\mathbf{x},\sigma) = \frac{1}{2}\sum_{i=1}^{2} w(b_i) b_i . \qquad (1)$$

Here, R_0 is the weighted medialness function and its variables are the position of each pixel ($\mathbf{x}$) and the scale σ. $w(b)$ is the weighting function and b_i is a 2D function defined as follows:

$$b_{1,2} = \nabla I^{(\sigma)}(\mathbf{x} \pm \theta\sigma\mathbf{v}_1) \qquad (2)$$

where $\nabla I^{(\sigma)}(\mathbf{x})$ is a boundaryness function and is equivalent to the amount of gradient of the pixel ($\mathbf{x}$) in the image convolved with a Gaussian kernel with a standard deviation of σ. v_1 is the eigen-vector related to the largest eigenvalue of Hessian matrix, and θ is a constant coefficient that defines as the relation of the radius of the vessels and the scale at which it should be detected.

Moreover, $w(b)$ used in this application is an exponential function shown by the following formula:

$$w(b_i) = \exp\left(-\left(1 - \frac{b_i}{0.5\times(b_1 + b_2)}\right)/(2\times\sigma^2)\right) \qquad (3)$$

Since retinal vessels are symmetric structures and the intensity of vessel section is estimated by the Gaussian function, choosing weighting function as shown in equation (3) operates as a matched filter and then intensifies the results of vessel's structures and weakens other structures.

To reduce the background noise, we use an adaptive thresholding using the gradient $\nabla I^{(\sigma)}$.

$$R(\mathbf{x},\sigma) = \begin{cases} R_0(\mathbf{x},\sigma) - \nabla I^{(\sigma)}(\mathbf{x}) & \text{if} \quad R_0(\mathbf{x},\sigma) > \nabla I^{(\sigma)}(\mathbf{x}) \\ 0 & \text{else} \end{cases} \qquad (4)$$

Since the amount of R_0 near of main axis of vessels is greater than $\nabla I^{(\sigma)}$, the medial-lines of vessels are enhanced after applying this function. Final result is then obtained by maximizing the response of medialness function in different scales as follows:

$$R_{multiscale} = \max_{scale}(R_{scale}(x,\sigma)) \qquad (5)$$

Although, the adaptive thresholding shown in equation (4) alleviates the background noises, it attenuates the response of vessels pixels. Therefore, employing the eigenvalues of the Hessian matrix, having strong response in the vessels, can reduce this effect. In order to reduce the impact of the image nonuniformity, we first convolve the sum of the eigenvalues with a Gaussian kernel. Then, with multiplying the consequent image by the multi-scale medialness function's response, the vessels are properly enhanced. Therefore, the final vessel medialness detection filter is obtained by:

$$R_{medial} = R_{multiscale} \times (Gaussian * (\lambda_1 + \lambda_2)) \qquad (6)$$

Fig. 2(b) illustrates the result of applying the vessel medialness detection filter on a retinal image. It is obvious that this filter properly extracts the line-like structures from the image.

2.2. Vessel Reconstruction

In this phase, the final segmentation result is attained by extracting centerline of vessels and estimating radius of vessels simultaneously.

2.2.1. Centerline Extraction

The main idea of centerline extraction step is to provide an impeccable vessel's centerlines. In this paper, three subsections including post processing, skeletonization and reconnection are applied for this purpose.

Noting this fact that the result of the previous phase is not infallible and noise-free, using post processing step in order to reduce the noise and abate the complexity of next steps, especially the reconnection step, is imperative. Since noisy pixels are usually round and small while fine vessels are elongated and larger than noises, we apply a post processing step which removes regions based on their area and elongation. In fact, the structures are classified to the noise and vessels with two features of area and elongation. If these parameters for a component are smaller than predefined thresholds, we presume it as a noise and remove it from the image. Using this assumption, the small vessels and capillaries are properly remained after this step.

In spite of attempting to keep vessels and remove noise, a vascular network with some disjoint points is remained after the post processing step. In order to connect these disjoint points, a reconnection step is used. For this purpose, first, the skeleton of vascular network is extracted. Then, by considering structural characteristics of retinal vessels,

image information and applying some constraints such as radius and slope changing constraint in potentially truncated vessels, the reconnection step is performed. The final result of centerline extraction step is demonstrated in Fig. 2(c).

2.2.2. Vessel Radius Estimation

To estimate the radius of vessels, we use information construed from each step of phase 1. Since each vessel with a specific radius appears better in a particular scale of medialness function, we can ascribe a unique radius ($R1 = \theta\sigma$) to each scale. *R1* describes maximum symmetrical radius which an object can have in a particular scale. On the other hands, the eigenvalues can congruously delineate the edges of vessels that can be used for estimating radii (*R2*) of vessels. By comparison of two radii (*R1* and *R2*), we can discriminate between vessels and abnormal regions and estimate an exact radius for a vessel. Since abnormal regions are usually asymmetric structures, If *R2* is much larger than *R1*, this structure will be an abnormal region and no radius is estimated for this region; otherwise, *R2* is selected as radius of vessel. Using this estimation and centerlines, the final result for segmentation of retinal vessels is attained (Fig. 2(d)).

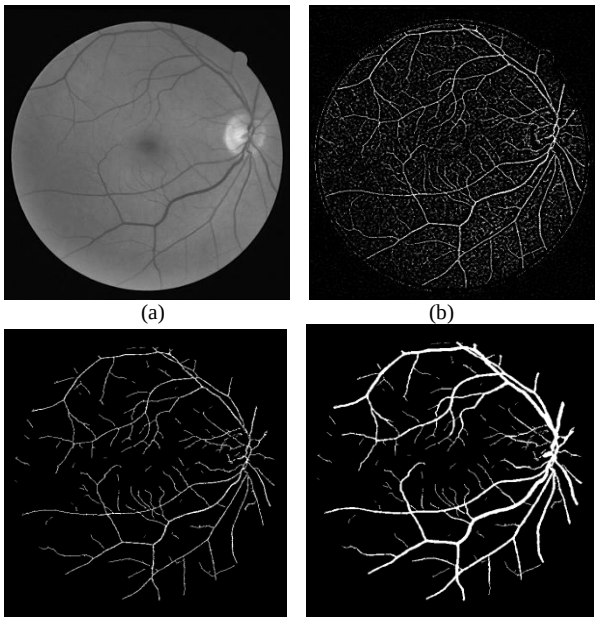

Fig. 2. (a) Green channel of the original image, (b) vessel medial-line extraction, (c) centerline extraction, (d) final result.

3. EXPERIMENTAL RESULTS

Our proposed method was tested on the images of two publicly available DRIVE and STARE databases, collected by Niemeijer *et al.* [9] and Hoover *et al.* [2], respectively. The DRIVE database contains 40 color images of the retina, with 565 × 584 pixels. A mask is provided for each image of this database in order to demarcate FOV. The database also consists of binary images with the results of manual segmentation. The 40 images were divided into a training set and a test set by the authors of the database. The second database, STARE database, includes 20 images with size of 650 × 550. For all of images in this database, a FOV of 650 × 550 pixels in the images has been supposed and two observers manually segmented all of these 20 images.

To evaluate our results, segmentation accuracy is opted as one of the performance measures. The accuracy is estimated by the ratio of the total number of correctly detected pixels as vessel and background (sum of true positives and true negatives) by the whole number of pixels inside the image FOV. Furthermore, the ROC curve is sketched in order to compare our results with other retinal vessel segmentation methods. In an ROC curve, the true positive rate (TPR) versus false positive rate (FPR) is plotted. Another performance measure reported in this paper is the area under the curve (AUC), calculated using ROC.

In Fig. 3, The ROC curves of DRIVE and STARE databases for some recent methods have been compared with our ROC curve.

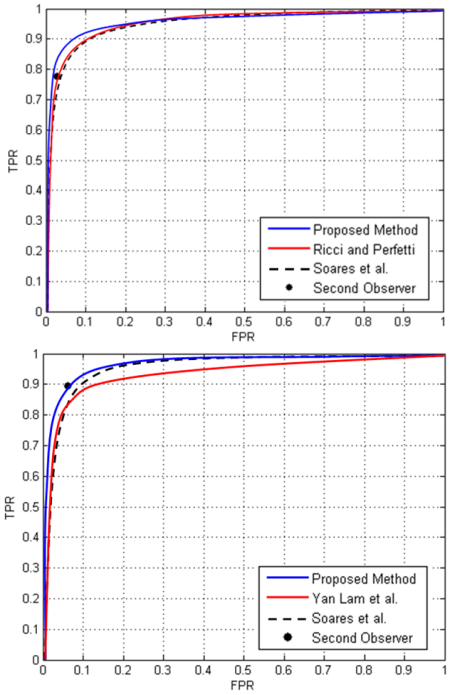

Fig. 3. The ROC curves of DRIVE (up) and STARE (down) database for different methods.

Also, in Table I, the average of accuracy and area under ROC of some methods, including our methods, for the 20 images of DRIVE's test set and the 20 images of STARE's dataset have been represented.

TABLE I
PERFORMANCE OF VESSEL SEGMENTATION METHODS

	DRIVE		STARE	
	Accuracy	AUC	Accuracy	AUC
2nd-observer	0.9473	-------	0.9354	------
Multi-scale	0.9659	0.9580	0.9756	0.9678
Ricci et al.[17]	0.9595	0.9633	0.9646	0.9680
Soares et al.[15]	0.9466	0.9614	0.9480	0.9671
Mendonça et al.[7]	0.9463	------	0.9479	------
Yan Lam et al.[22]	-------	------	0.9474	0.9392

According to sharp slope of both of our ROC curves in Fig. 3, we can infer that the algorithm can reach high TPR

while maintain FPR low. Also, in Table I, it is obvious that the average accuracy of the multi-scale method for both databases is comparable to other methods. In fact, it takes place due to high value of TPR along with low value of FPR. Therefore, it can be concluded that one of salient features of this method is to eschew detecting false vessels, occurred due to noise or pathological abnormality. Another discussable point regarding this table is that the area under ROC is comparable with other methods, especially in STARE dataset. Actually, because of presence of more pathological regions in STARE's images, our proposed scheme can better avoid detecting false regions as vessel and function more reliably.

In order to prove our claims graphically, in Fig. 4, result of our method versus the result of Ricci *et al.* [5] on an image of DRIVE dataset is demonstrated. As it is obvious, the circle around the blind spot has properly been removed using the multi-scale method.

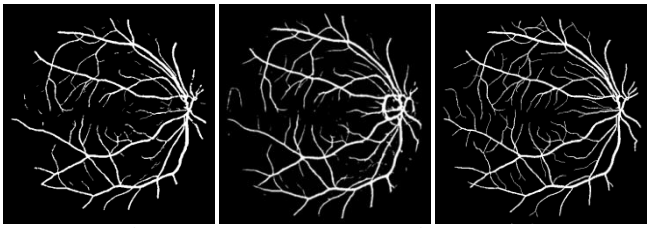

Fig. 4. From left to right: segmentation results of the Multi-scale approach, Ricci *et al*. method, and Manual segmentation of observer A.

Fig. 5 is another example concerning an image from the STARE database with some abnormal regions stuck the vessel's areas. In this situation, the multi-scale method has congruously found vessels in the midst of abnormal regions. Although some vessels have been truncated in these regions, reconnection step revived some connections of vessels. Totally, this method reached agreeable result compared to the results of Soares *et al.* and Yam Lam *et al.*

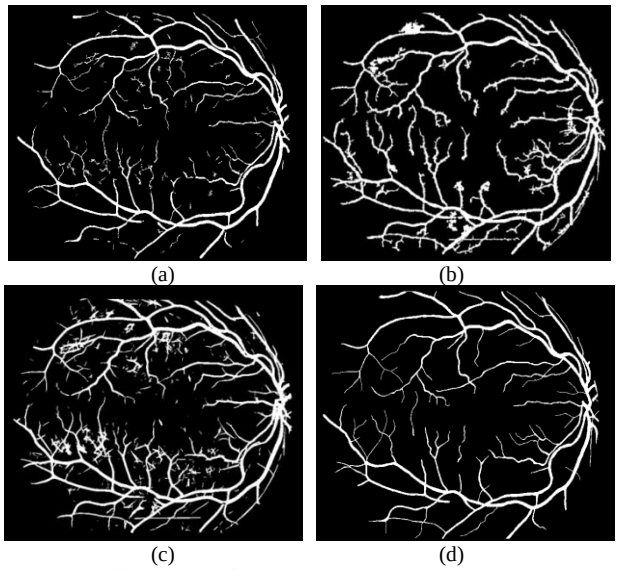

Fig. 5. Results for an image from the STARE dataset, (a) Proposed method, (b) Yan Lam *et al.*, (c) Soares *et al.*, (d) Ground truth 1.

4. DISCUSSION AND CONCLUSION

In this paper, a new approach based on a multi-scale method for segmentation of retinal vessel was proposed. Using a weighted medialness function along with the eigenvalues of the Hessian matrix facilitates detection of vessel structures whilst reduces the response of this function for asymmetric structures which usually are not vessels.

Moreover, other steps such as post processing, reconnection and radius estimations appropriately affect the amounts of FPR and TPR and consequently the final results of segmentation. Therefore, it can be concluded that the main characteristic of this method compared to other recent methods is to better avoid detecting false vessels.

Notwithstanding mentioned advantage, it seems that our method cannot detect fine vessels as well as some recent methods (Fig. 5). It can be shown that some of fine vessels are removed by the post processing step and these vessels are not revived by the reconnection step; this can be supposed as a weakness of this scheme. As future work to address this problem, we can merge post processing and reconnection steps so that these steps operate simultaneously and decision about removing a region or connecting it to other region is made concurrently.

5. REFERENCES

[1] M. E. Martinez-Perez, A. D. Hughes, A. V. Stanton, S. A. Thom, N. Chapman, A. B. Bharath, and K. H. Parker, "Retinal vascular tree morphology: A semi-automatic quantification," *IEEE Trans. Biomed. Eng.*, vol. 49, no. 8, pp. 912–917, Aug. 2002.

[2] A. Hoover, V. Kouznetsova, and M. Goldbaum, "Locating blood vessels in retinal images by piecewise threshold probing of a matched filter response," *IEEE Trans. Med. Imag.*, vol. 19, no. 3, pp. 203–210, Mar. 2000.

[3] B. Al-Diri, A. Hunter, and D. Steel, "An active contour model for segmenting and measuring retinal vessels," *IEEE Trans. Med. Imag.*, vol. 28, no. 9, pp. 1488–1497, Sep. 2009.

[4] J. V. B. Soares, J. J. G. Leandro, R. M. Cesar, Jr., H. F. Jelinek, and M. J. Cree, "Retinal vessel segmentation using the 2D Gabor wavelet and supervised classification," *IEEE Trans. Med. Imag.*, vol. 25, no. 9, pp. 1214–1222, Sep. 2006.

[5] E. Ricci and R. Perfetti, "Retinal Blood Vessel Segmentation Using Line Operators and Support Vector Classification, " *IEEE Trans. Med. Imag.*, vol. 26, no. 10, pp. 1357–1365, Oct. 2007.

[6] A. M. Mendonça and A. Campilho, "Segmentation of retinal blood vessels by combining the detection of centerlines and morphological reconstruction," *IEEE Trans. Med. Imag.*, vol. 25, no. 9, pp. 1200–1213, Sep. 2006.

[7] B. S. Yan Lam and H. Yan, "A novel vessel segmentation algorithm for pathological retina images based on the divergence of vector fields," *IEEE Trans. Med. Imag.*, vol. 27, no. 2, pp. 237–246, Feb. 2008.

[8] T.G. Pock, "Robust segmentation of tubular structures in 3D volume data", *M.S. Thesis*, University of Graz, 2004.

[9] M. Niemeijer, J. Staal, B. van Ginneken, M. Loog, and M. D. Abramoff, "Comparative study of retinal vessel segmentation methods on a new publicly available database," in *SPIE Med. Imag.*, J.M. Fitzpatrick and M. Sonka, Eds., 2004, vol. 5370, pp. 648–656.